



Predicting the Stress and Deformation of Pump-turbine's Guide Vane at Small Opening

Zhiyu Tao, Mingkun Fang, Ran Tao*

College of Water Resources and Civil Engineering, China Agricultural University,
Beijing 100083, China

*Corresponding author's e-mail: randytao@cau.edu.cn

Abstract. Guide vane is a key component of reversible pump-turbine for flow regulation and guidance. In the start-up process of pump mode, guide vane will be closed for a long time until runner rotates in full speed and then continually opens maximum. When the opening angle is small, guide vane suffers large and pulsating hydraulic force due to complex transient flow regime. The stress and deformation of guide vane are important when considering the hydraulic stability of pump-turbine. In this study, computational fluid dynamics analysis is conducted under 10% maximum guide vane opening angle based on simplified domain. The jet-vortex flow structure can be observed in guide vane and stay vane and induces pulsating torque on guide vane blade. The stress and deformation of guide vane are studied by fluid-solid interaction method at torque peak, middle and valley conditions. The structural response characteristics are understood at small opening angle condition and can be referred for full operation conditions. This study provides a fast prediction way of the structural response of guide vane which is suitable for engineering cases and generates the typical force variation law for referring.

Keywords: pump-turbine; guide vane opening; stress; deformation

1 Introduction

Reversible pump-turbine is the key component in pumped storage power station. It has two stage radial vanes including guide vane and stay vane for flow regulation and guidance^[1]. In the starting and stopping process, guide vane will be in small opening. Flow is strongly prevented by guide vane and becomes undesirable^[2]. Many researchers studied the flow case at small guide vane opening. Flow instability, stall in vaneless region, inter-vane jet and other relevant problems were pointed out^[3-6]. Huge pressure difference was found between the front and back side of the small opening guide vane blade. Based on experience, the huge pressure difference may cause high stress and deformation on turbomachinery blades^[7]. Plastic deformation and fatigue failure should be cautioned. In this study, a prototype scale reversible pump turbine is selected as the research objective and the guide vane's structural response problem is mainly focused on. Generally, the structural response including the force, stress and

© The Author(s) 2025

Y. Qiu et al. (eds.), *Proceedings of the 2024 7th International Conference on Civil Architecture, Hydropower and Engineering Management (CAHEM 2024)*, Advances in Engineering Research 256, https://doi.org/10.2991/978-94-6463-650-5_6

deformation are analysed on the guide vane based on fluid-solid interaction. The condition is extremely off-design with very small guide vane opening which means that the guide vane will face a complex excitation force. This study will help enhancing the operation stability of pumped storage unit.

2 Studied Object and Simulation Setup

2.1 Parameters of Pump-turbine

In this study, a reversible pump turbine unit is studied in pump mode. It has a 9-blade runner, 20-blade guide vane and 20-blade stay vane. This pump turbine is under the rotation speed of 430 rpm. The diameter at runner high-pressure side D_{hi} is 4.16 m. The dimensionless flow rate coefficient C_ϕ and head coefficient C_ψ are defined as:

$$C_\psi = \frac{2gH}{\omega^2 R_{ref}^2} \quad (1)$$

$$C_\phi = \frac{Q}{\pi\omega R_{ref}^3} \quad (2)$$

where g is the acceleration of gravity, H is the head, Q is flow rate, ω is the rotational angular speed, R_{ref} can be $0.5 D_{hi}$. The flow rate coefficient C_ϕ and head coefficient C_ψ at best efficiency point are 0.043 and 1.051.

2.2 Flow Domain and Structure Domain

In this study, the condition with small guide vane opening is analyzed. The guide vane opening angle is 3 degrees which is about 10% of the maximum opening angle. It represents the very small opening with probably local submerged jet flow which is the main cause of flow field pulsation. The flow rate coefficient C_ϕ is 0.015. Figure 1 shows the flow domain using in the computational fluid dynamics (CFD) simulation. It includes the draft tube, runner, guide vane and stay vane. To simplify the simulation, the draft tube was modelled with only $0.25 D_{hi}$ length between runner and inlet boundary. The runner domain is one single blade passage. The guide vane and stay vane domain are also single blade passages. Outlet boundary is set at the outflow of stay vane passage. The flow domain has 155611 mesh node in total. Figure 2 shows the structure domain of guide vane for predicting the stress and deformation by fluid-solid interaction (FSI) simulation. The structure domain has 95061 nodes in total.

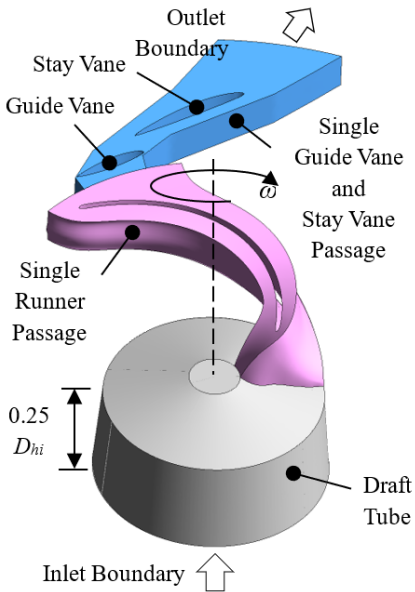


Fig. 1. Flow domain of draft tube, runner and vanes

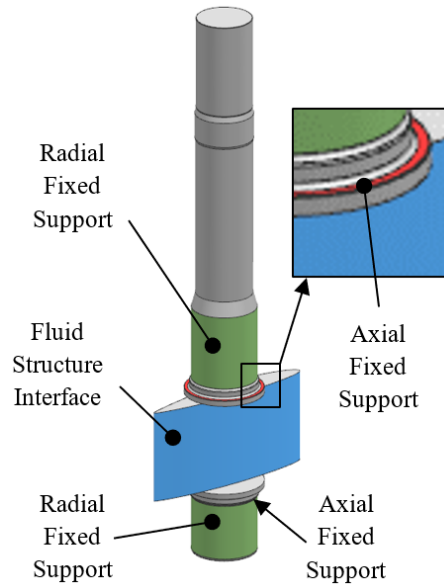


Fig. 2. Structure domain of guide vane

2.3 CFD and FSI Setup

The CFD simulations are conducted in transient state based on the flow domain in Fig. 1. The commercial software ANSYS CFX is used. The fluid medium is set as water at 20 °C. The reference pressure is set as 1 Atm. Mass flow inlet boundary is given at the inlet boundary site shown in Fig. 1. Pressure outlet boundary is given at the outlet boundary site shown in Fig. 1. Rotational periodic boundaries are given to simplified the single blade passages. Domain interfaces are given for connecting different domains. The continuity, momentum and total energy equations are solved for predicting the flow field. The SST turbulence model [8] is used based on the Reynolds averaged Navier-Stokes equations. This is a zonal hybrid model which treats both the near-wall flow and main flow well based on a lot of actual engineering simulation cases. The steady state simulation is conducted up to 600 iterations as the initial condition of transient simulation. The transient simulation is conducted for totally 10 runner revolutions. 360 steps are taken in each revolution with maximum 10 iterations for each step. The convergence criterion is that the root-mean-square (RMS) residuals become less than 1×10^{-5} .

In the FSI simulation, the flow field are loaded on the guide vane for simulating the stress and deformation. The hydraulic force solved in CFD simulation can be loaded on the fluid structure interface of guide vane (vane blade surface shown in Fig. 2) by

interpolation. The radial fixed supports are given on the surfaces surrounded by radial bearings as shown in Fig. 2. The axial supports are given on the surfaces of vane ring as also shown in Fig. 2. The stress and deformation can be solved based on the linear structural transient power balance equation [9]. The von Mises equivalent stress can be calculated based on the fourth strength theory.

3 Results and Analysis

3.1 Internal Flow in Runner and Vanes

The absolute velocity vectors in runner and vanes are plotted on the spanwise 0.5 surface as shown in Fig. 3. The vectors are colored by velocity coefficient C_v :

$$C_v = \frac{V_{abs}}{V_{in}} \quad (3)$$

where V_{abs} is the absolute velocity, V_{in} is the average absolute velocity at inlet boundary.

In Fig. 3, water ring can be found between runner trailing-edge and guide vane. It forms because of the small guide vane opening. Most of the water are prevented from passing through the guide vane. However, some water flow across the inter guide vane leakage and generate jet flow. Between two jets, vortices can be observed on the back side of guide vane. Another large scale vortex can be found in the stay vane passage. Based on the flow regime shown in Fig. 3, the flow around guide vane is strongly pulsating.

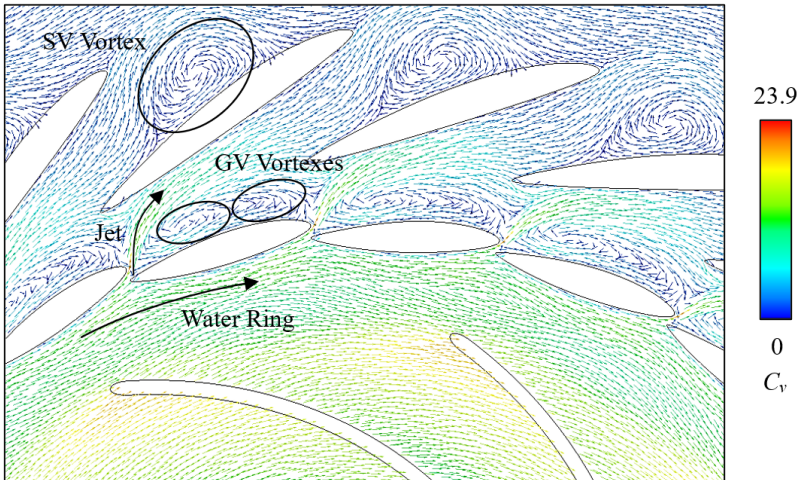


Fig. 3. Velocity vector on the spanwise 0.5 surface in runner and vanes

3.2 Torque on Guide Vane

To analyse the influence of pulsating flow on guide vane, the torque on guide vane T_{gv} is monitored based on the axis shown in Fig. 4. The positive and negative value of T_{gv} are indicated. The leading-edge (LE) and Trailing-edge (TE) are also defined and illustrated for pump mode.

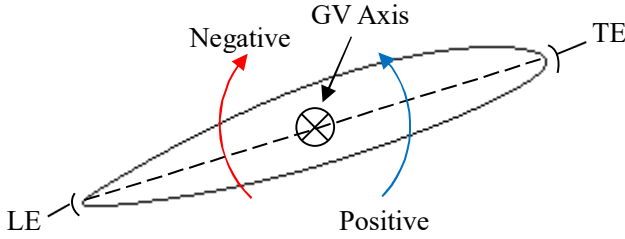


Fig. 4. Definitions for monitoring the torque on guide vane

Figure 5 shows the pulsation of T_{gv} within 3 runner revolutions. The frequency-domain plot is based on the Fast Fourier Transformation (FFT). The value of T_{gv} pulses from about -35516 N·m to about -42596 N·m by mainly the frequency $f_{rm}=7.16$ Hz. This frequency is the runner rotation frequency. Three timesteps that negative valley (#1), middle (#2) and negative peak (#3) of T_{gv} are chosen for comparison.

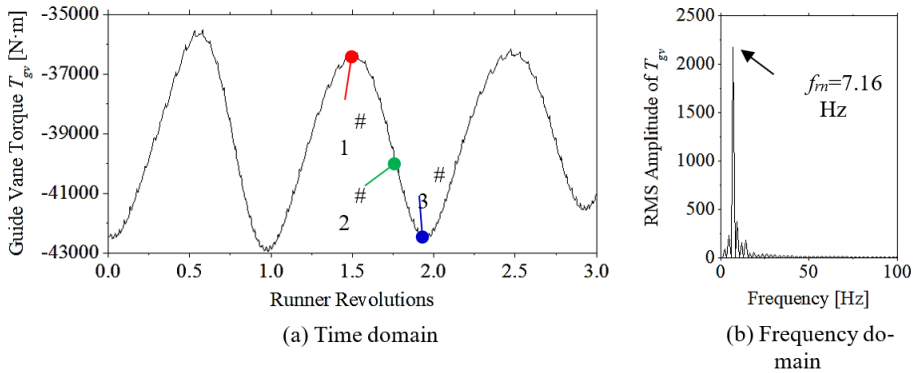


Fig. 5. Monitoring of the torque on guide vane T_{gv}

Figure 6 shows the flow regime and force F around guide vane around guide vane. The force F on the front surface of guide vane strongly varies during runner rotation. The torque T_{gv} reaches the negative peak value when F is big on the front surface near LE. On the contrary, the torque T_{gv} reaches the negative valley value when F becomes small on the front surface near LE. Thus, the periodic striking of the water ring flow is the main reason of guide vane torque. On the back surface of guide vane, the force F and the vortex structure are also periodic changing. At the negative peak (#3) point, the

vortex on the guide vane back surface is one. At the middle (#2) point, another small vortex occurs near LE. At the negative valley (#1) point, there are two equal-scale vortices can be observed. The force produced by each vortex becomes weaker. The force changing on the back surface of guide vane also influences T_{gv} .

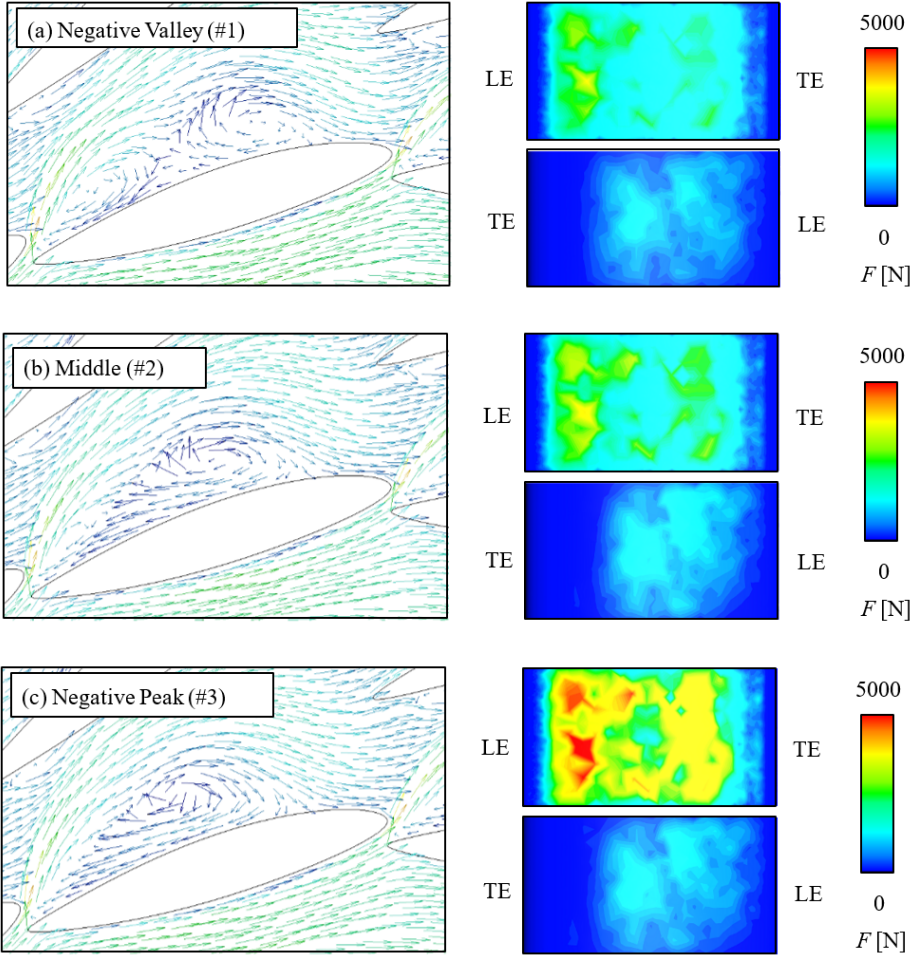


Fig. 6. Flow regime and force F around guide vane

3.3 Stress and Deformation on Guide Vane

The stress and deformation will be induced by the force on guide vane. Figure 7 shows the contour of stress and deformation. The maximum stress is on the connection between guide vane blade and shaft. The maximum deformation is on the blade leading-edge where is also the high force region. The blade trailing-edge is also in large deformation.

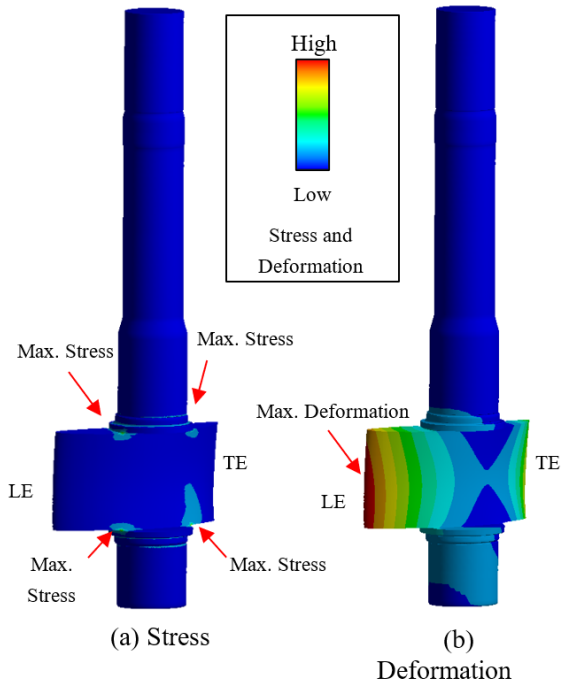


Fig. 7. Stress and deformation contours

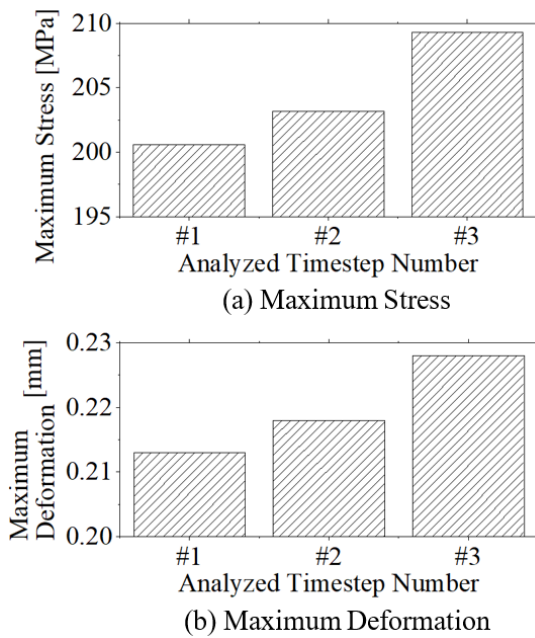


Fig. 8. Maximum stress and deformation values

Figure 8 shows the maximum stress and deformation values at negative valley (#1), middle (#2) and negative peak (#3) timestep points. The maximum stress among the three timesteps is at #3, it is about 209.3 MPa. The minimum stress among the three timesteps is at #1, it is about 200.6 MPa. The maximum deformation on guide vane blade can be from 0.213 mm to 0.228 mm. The maximum stress does not exceed the allowable stress that 235 MPa. However, the variation of stress need further checks for avoiding the fatigue failure.

4 Conclusions

In this study, the flow regime in pump-turbine is studied in pump mode at small guide vane opening. The force, stress and deformation on guide vane are analyzed with conclusions drawn as follows:

1) At small guide vane opening, jet flow generates in the inter guide vane leakage. Vortexes can be found on the back side of guide vane and in the stay vane passage. This jet-vortex flow structure is strongly pulsating and may excite fluctuating hydraulic force.

2) The torque on guide vane is monitored during runner rotating. The torque value pulses from about $-35516 \text{ N}\cdot\text{m}$ to about $-42596 \text{ N}\cdot\text{m}$ by mainly the frequency of 7.16 Hz. This specific frequency is the runner rotating frequency. The force on guide vane blade periodically changes and induces varying torque. It proves that the runner incoming flow will strongly impact the guide vane at small opening angle.

3) The stress and deformation on guide vane also periodically change during runner rotation. The maximum stress varies from 200.6 MPa to 209.3 MPa at the connection between blade and shaft. The maximum deformation varies from 0.213 mm to 0.228 mm at guide vane leading-edge. Fatigue failure at the maximum stress site should be cautioned.

These above conclusions will help improving the operation stability and security especially in the start up or shut down process of pump turbines with small guide vane angle. It helps the future design and operation strategy of pumped storage hydropower technique which is a support of green development.

Acknowledgements

The authors would like to acknowledge the support of China Postdoctoral Science Foundation No. 2018M640126 and National Natural Science Foundation of China No. 51909131.

References

1. Tanaka H, Tsunoda S. The development of high head single stage pump-turbines. *Proceedings of the 10th IAHR Symposium on Hydraulic Machinery and Cavitation*, 1980, Tokyo, Japan.

2. Mei Z. *Technology of Pumped-Storage Power Generation*. China Machine Press, 2000.
3. Nennemann B, Parkinson E. Yixing pump turbine guide vane vibrations: problem resolution with advanced CFD analysis. *IOP Conferences Series: Earth and Environmental Science*, 2010, 12: 012057.
4. Braun O, Kueny J L, Avellan F. Numerical analysis of flow phenomena related to the unstable energy-discharge characteristic of a pump-turbine in pump mode. *ASME 2005 Fluids Engineering Division Summer Meeting*, 2005, Houston, USA.
5. Zhu D, Xiao R, Tao R, *et al*. Impact of guide vane opening angle on the flow stability in a pump-turbine in pump mode. *Proceedings of the Institution of Mechanical Engineers Part C: Journal of Mechanical Engineering Science*, 2016, 231(13): 2484-2492.
6. Li D Y, Gong R Z, Wang H J, *et al*. Numerical investigation in the vaned distributor under different guide vanes openings of a pump turbine in pump mode. *Journal of Applied Fluid Mechanics*, 2016, 9(1): 253-266.
7. Presas A, Luo Y, Wang Z, *et al*. Fatigue life estimation of Francis turbines based on experimental strain measurements: review of the actual data and future trends. *Renewable and Sustainable Energy Reviews*, 2019, 102: 96-110.
8. Menter F R, Kuntz M, Langtry R. Ten years of industrial experience with the SST turbulence model. *Turbulence, Heat and Mass Transfer*, 2003, 4(1): 625-632.
9. Xiao R, Wang Z, Luo Y. Dynamic stresses in a francis turbine runner based on fluid-structure interaction analysis. *Tsinghua Science and Technology*, 2008, 13(5): 587-592.

Open Access This chapter is licensed under the terms of the Creative Commons Attribution-NonCommercial 4.0 International License (<http://creativecommons.org/licenses/by-nc/4.0/>), which permits any noncommercial use, sharing, adaptation, distribution and reproduction in any medium or format, as long as you give appropriate credit to the original author(s) and the source, provide a link to the Creative Commons license and indicate if changes were made.

The images or other third party material in this chapter are included in the chapter's Creative Commons license, unless indicated otherwise in a credit line to the material. If material is not included in the chapter's Creative Commons license and your intended use is not permitted by statutory regulation or exceeds the permitted use, you will need to obtain permission directly from the copyright holder.

